We are IntechOpen, the world's leading publisher of Open Access books Built by scientists, for scientists

4,800
Open access books available

122,000
International authors and editors

135M
Downloads

Our authors are among the

154
Countries delivered to

TOP 1%
most cited scientists

12.2%
Contributors from top 500 universities

CLARIVATE ANALYTICS
BOOK CITATION INDEX
INDEXED

WEB OF SCIENCE™

Selection of our books indexed in the Book Citation Index
in Web of Science™ Core Collection (BKCI)

Interested in publishing with us?
Contact book.department@intechopen.com

Numbers displayed above are based on latest data collected.
For more information visit www.intechopen.com

Inductive Telemetric Measurement Systems for Remote Sensing

Daniele Marioli, Emilio Sardini and Mauro Serpelloni
Department of Information Engineering:
Electronics, Informatics, Telecommunications and Control,
University of Brescia
Italy

1. Introduction

Inductive telemetric measurement systems can be used for contactless measurement using passive sensors that may be interrogated by an external unit without a physical contact.

The main appealing features with respect to traditional sensors come from the absence of any cable linking to the acquisition unit, the reduced ecological impact, since they are battery-less, and from the extension of their application fields from traditional to harsh environments. Inductive telemetric systems can be adopted in situations where the measurement information should be acquired or in presence of incompatibility with the electronics requirements or in inaccessible environments.

Their use widens to applications where wires, connecting a data acquisition unit and the sensor element, cannot be used such as, for examples, in implantable devices inside the human body to avoid risk of infections or skin damage or in hermetic environments.

Inductive telemetric systems are applied in industrial fields, for example, when the measuring environment is not accessible, since inside, for example, a hermetic box. Other typical applications are measurement of physical quantities in environments at high temperature where it is not possible to use silicon microelectronic circuits, with consequent unavailability of active blocks within the sensing head for the electronic processing and transmission of the signals. In this case the sensor can be only of passive type and requires to be interrogated contactless.

A solution can be offered sometimes by standard wireless techniques that anyway does not present, in many cases, a definitive solution, because the wireless electronic circuits need powering energy supplied by a battery that can periodically be substituted. Furthermore, exhausted batteries are important environmental problems and they require appropriate disposal. In the previous examples, inductive telemetric measurement systems can represent a valid solution, since they do require neither connections through cables or electronic circuits to process and transmit the signal and avoids the use of batteries.

Inductive telemetric measurement systems are usually constituted by two inductors: one (sensing inductor) connected to the sensitive element, commonly a capacitive transducer, and the other to the measurement circuit (readout inductor).

Different examples of application using the telemetric measurement system are reported in the literature. In (Fonseca et al., 2002), the telemetric system is used to monitor the pressure inside high temperature environments. In (Hamici et al., 1996), an example in the field of biomedical applications for the monitoring of internal package humidity for either in vitro or in vivo testing is described. The system consists of a high-sensitivity capacitive humidity sensor that forms an LC tank circuit together with a hybrid coil wound around a ferrite substrate. The resonant frequency of the circuit depends on the humidity sensor capacitance. This sensor uses the hybrid coil for coupling through the magnetic field with an external inductor, and then the information of humidity is transduced to outside the package.

Another example of humidity monitoring using a passive telemetric system is quoted in (Harpster et al., 2002). The proposed telemetric technique advantageously allows the insertion of a cheap sensor inside every package and executes the measurement without the necessity of opening the hermetic box.

Inductive telemetric measurement systems are also adopted in many other fields: in the literature, several applications in harsh environments are described, such as under high temperatures, cold, humidity or corrosive conditions (Akar et al., 2001; Todoroki et al., 2003; Birdsell et al., 2006; Jia et al., 2006, Tan et al., 2007). Furthermore, examples of inductive telemetric measurement systems for biomedical applications are reported in (Fonseca et al., 2006; Schnakenberg et al., 2000).

In (Takahata et al., 2008) the coil core of a wire wound inductor is a micromachined capacitive pressure device; the sensor operates in harsh or protected environments and can be remotely interrogated by a wireless setup. The inductive telemetric system has been tested in a plastic chamber full of water; the resonant frequency of the tank is monitored outside by an antenna connected to an impedance analyzer. In (Ong et al., 2001) a system for environmental wireless monitoring consists of a LC sensor and two loop antennas (transmitter and receiver). A change of the L and/or C parameters is reflected as mutual impedance on the receiver antenna.

This chapter is basically aim at describing telemetric systems, their electrical models and the measurement techniques used. Then a general architecture of an inductive telemetric system is presented.

The model and its simplified version are shown and two measurement techniques that offer different performance characteristics are reported. Furthermore, an electronic circuit that implements the technique fullest extent is described and tested. Finally, the chapter reports two applications for harsh or hermetic environments: two examples of passive sensors that are related by an inductive telemetric system are described, the first one for humidity measurements and the second for high temperatures. The first application is the measurements of relative humidity in hermetic environments, for example in logistic and biomedical fields. The second application is the temperature monitoring of an isolated system inside a harsh environment, like ovens.

The telemetric temperature systems can be a solution for measurements into harsh or hermetic environments, thereby eliminating the need for physical contacts, active elements, or power supplies, which cannot withstand harsh or hermetic environments.

2. Architectures and Measurement Techniques

2.1 Telemetric System

This section describes an inductive telemetric measurement system and its components. Inductive telemetric measurement systems have the capability, through an inductive coupling, to link wirelessly two devices, one of them being just a passive element. A general architecture of a telemetric measurement system is schematically shown in Figure 1.
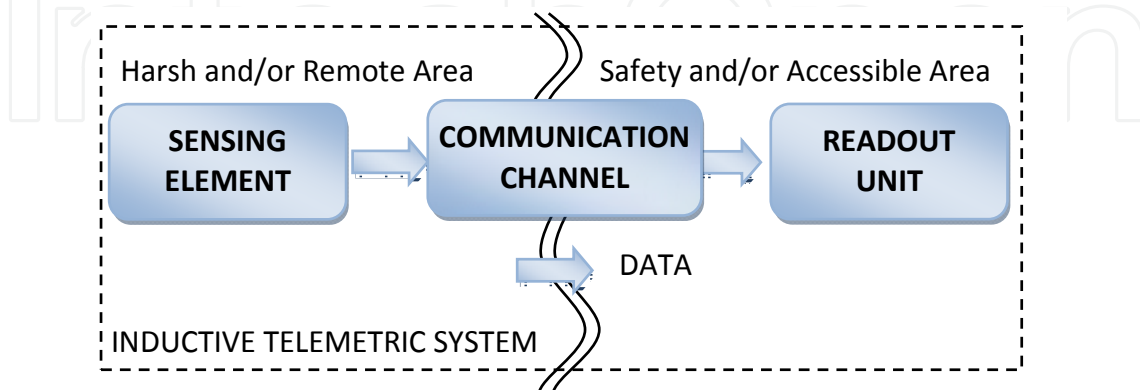

Fig. 1. General architecture of a telemetric system.

Basically it is a measurement system with two different areas: the harsh and/or remote area, where the sensing element transduces the quantity under measurement and the safety or accessible area, where the read out unit is hosted. Between the sensing element and the readout unit there is usually a barrier separating the two areas. The sensing element and the readout unit are connected by a wireless communication channel that uses a magnetic link. The measurement information is acquired by the sensing element, sent through the communication channel using the magnetic coupling, read as reflected impedance by the conditioning electronics and elaborated by the readout unit. The characteristics of the barrier material (mainly material type and dimensions) influence the system's performance. A strong influence is due to the conductive property of the material; it constitutes a serious obstacle since the induced eddy currents reduce the magnetic field amplitude. The frequency of the magnetic field depends on the specific application: different examples of telemetric systems use frequencies ranging from hundreds up to tens of Mega Hertz.

As shown in Figure 2, an inductive telemetric system consists of two inductors: one, labelled sensing inductor, is connected to the sensing element, and the other, readout inductor, to the readout unit. The two inductors are coupled by a magnetic field, and they are placed at a distance that can be fixed or can change. The sensing element is a passive device that, normally, does not require any additional power supply. The front-end electronic circuit is linked to the terminals of the read out inductor: the reflected impedance at these terminals is correlated by the quantity under measurement.
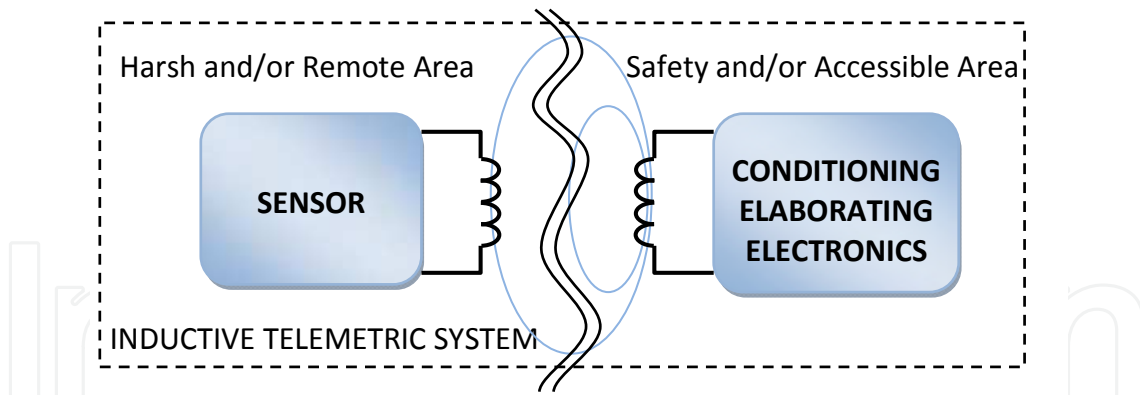
Fig. 2. General architecture of an inductive telemetric measurement system.

2.2 Model of the system

2.2.1 Physical model

Models of different complexity are reported in literature. For sake of completeness, a physical model should also include the effects of parasitic capacitances of each inductor, the coupling capacitance between the two inductors and the leakage magnetic fluxes. The reason to keep into consideration these elements are that the values of the parasitic elements can be equal to the value of the transducer capacitance, and a changing in the geometry of the system produces a change in the coupling and leakage fluxes.
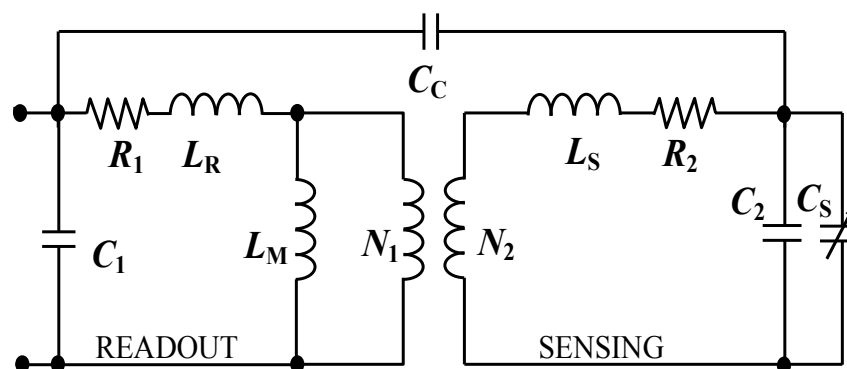
Fig. 3. The proposed physical model to analyze the inductive telemetric systems.

A physical model of an inductive telemetric system is shown in Figure 3. The parameters have the following meaning:

1) R_1, R_2 are the equivalent resistances of readout and sensor;
2) C_1, C_2 are the parasitic capacitances of the readout and sensor inductor respectively;
3) C_S is the sensor capacitance;
4) L_R, L_S are the readout and sensor leakage inductances;
5) L_M is referred to coupled flux;
6) N_1 and N_2 are the equivalent number of the inductor windings; they kept into considerations the possible different number of turns of each inductor.
7) C_C is the coupling capacitance.

The coupling capacitance C_C keeps into consideration the effects of the electric field coupled between the conducting tracks of the two inductors; its value is generally low even for close distances and can be further minimized increasing the distance between the two inductors. The coupling capacitance value depends on the inductor construction type and on the geometry. For coil inductors, the area faced between the two inductors is small and the coupling capacitance value is very low and can be neglected. Flat type inductors are different since the faced area can be very large. But also in this case, making the external diameter of the sensible inductor equal to the internal diameter of the readout inductor, the faced area can be reduced and the coupling capacitance can be neglected.
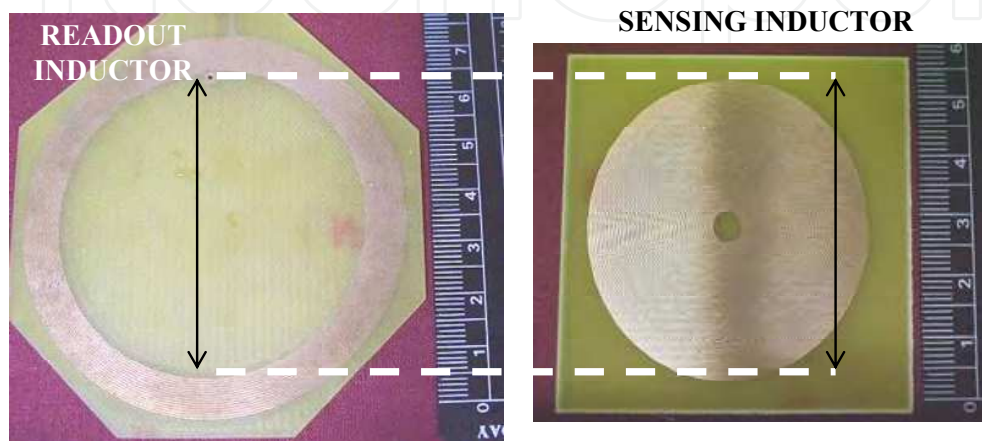

Fig. 4. The realized planar inductors.

An example of flat type inductors with an internal diameter of the readout inductor equal to the external diameter of the sensing inductor is reported in Figure 4. For these reasons, the coupling capacitance Cc can be neglected without loss of generality. Since the working frequency range is high, the resistances R_1, R_2 can be neglected since they have impedances of much less value than those of the series inductor L_R, L_S. The model of Figure 3 can be simplified into that shown in Figure 5, where the elements of the sensing circuit are brought to the readout circuit. L and C are L_S and C'_S as seen from the primary of the ideal transformer and parameter "n" is the ratio between N_1 and N_2. C'_S is the parallel of C_2 and C_S.
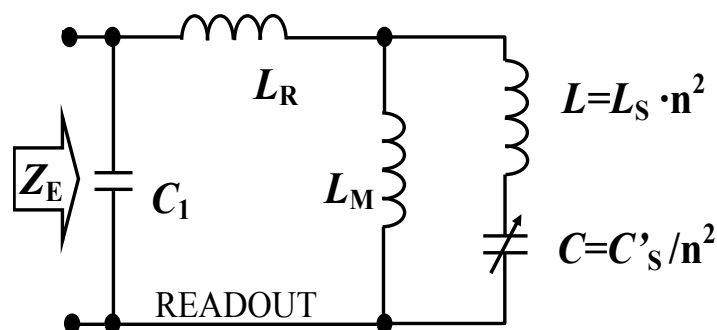

Fig. 5. A simplified version of Figure 3 without the coupling capacitance and the resistances.

If the simplified model is considered, the impedance at the terminal is:

$$Z_E(s) = \frac{s^3(L_M LC + L_R C(L_M + L)) + s(L_M + L_R)}{s^4 C_1(L_M LC + L_R C(L_M + L)) + s^2(C_1(L_M + L_R) + C(L_M + L)) + 1} \quad (1)$$

The impedance function of equation (1) has a diagram that agrees with the data obtained by experimental measurements. Figure 6 shows typical impedance measured on a real telemetric system and obtained when the measuring probes are applied to the readout circuit terminals. There are three noticeable frequencies f_{ra}, f_{rb} and f_a: f_{rb} is mainly due to the self resonance of the readout inductor. f_{min} is the frequency at which the phase of the impedance reaches its minimum as indicated in Figure 6.
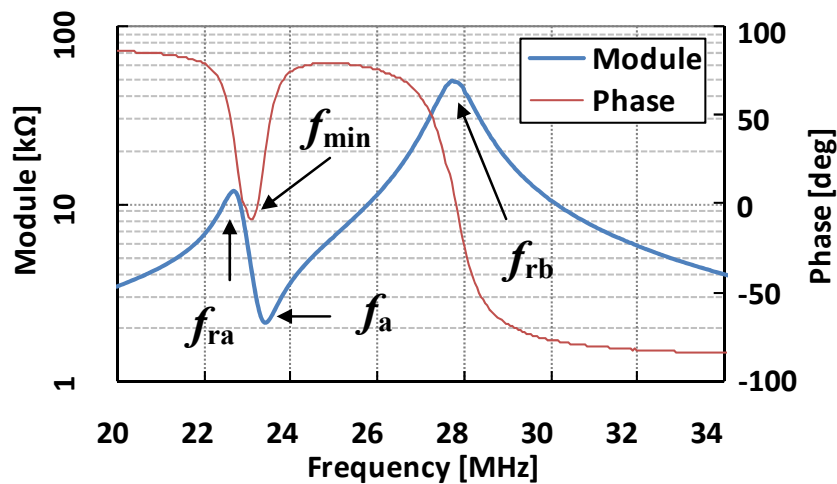

Fig. 6. Impedance as seen from the terminal of the readout inductance.

First (f_{ra}) and second resonant frequency (f_{rb}) have complicated expressions that are reported below (2) and (3). They are both influenced by C_1 and C. The resonant frequency (f_a) is influenced only by C and it is more sensitive to C than the other two frequencies. The expression for f_a, f_{ra} and f_{rb} are:

$$f_a = \frac{1}{2\pi\sqrt{C \cdot \left(L + \frac{L_M L_R}{L_R + L_M}\right)}} \quad (2)$$

$$(2\pi f_{ra,b})^2 = \frac{1}{2C\left(L + \frac{L_R L_M}{L_R + L_M}\right)} + \frac{1}{2C_1\left(L_R + \frac{L L_M}{L + L_M}\right)} \pm$$

$$\sqrt{\frac{1}{4C^2\left(L + \frac{L_R L_M}{L_R + L_M}\right)^2} - \frac{1}{4C_1^2\left(L_R + \frac{L L_M}{L + L_M}\right)^2} - \frac{L_M^2 - L_R L_M - L L_R - L L_M}{2CC_1(L L_R + L L_M + L_R L_M)^2}} \quad (3)$$

f_a depends on C, and also on distance, since the distance changes the inductance.

The other two frequencies (f_{ra} and f_{rb}) have dependence more complex and dependent also on the parasitic capacitance of the readout inductor C_1.

Because f_a depends only on the transducer capacitance, while f_{ra} and f_{rb} depend also on C_1, it seems more useful to measure f_a. A sensitivity analysis has been conducted on the equivalent system of the telemetric circuit with the simulation software PSpice using the circuit of Figure 5. The simulation results show that the changes of C influence both the three resonances, as expected, but with different sensitivity: the f_a resonance is more sensitive. A confirmation of the previous considerations can also be obtained by analyzing the experimental results reported in paragraph 4.

Anyway, even if the transducer capacitance is kept constant, but the distance between the readout and sensing inductances changes, the three resonant frequencies change. In fact, when the distance changes, the coupled and leakage flux change too modifying the value of L_M, L_R and L: for f_a this effect is clearly visible by analyzing the terms into parenthesis of equation 2. The results obtained from theoretical analysis are confirmed from experimental measurements.

2.2.2 Simplified model

A simplified model of a telemetric system is reported in Figure 7. This model neglects the parasitic capacitances and, also, the leakage fluxes and their changing due to a distance variation, but M coefficient keeps into consideration the coupled magnetic flux. Even if the two previously effects are neglected, the model can be accurately used in many applications when the transducer capacitance is much greater than the parasitic capacitance of the inductor and the distance between the two inductors is kept constant.
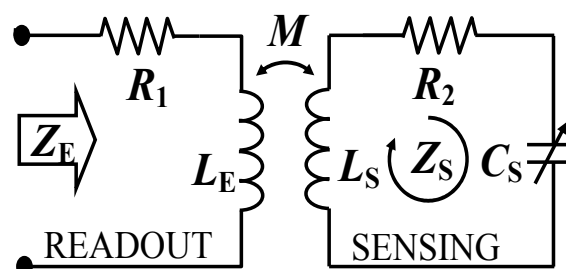

Fig. 7. A model, commonly used, to analyze telemetric systems.

Figure 7 reports the equivalent circuit: the planar inductance is modelled with an inductor (L_S), a series parasitic resistance (R_2) and a variable capacitor (C_S) representing the capacitance sensor. The readout circuit is modelled with an inductor (L_E) and a series parasitic resistance (R_1). When the two circuits are close, there is a mutual inductance coupling (M) between the inductor L_S and the inductor L_E.

2.3 Measurement techniques.

The measurement techniques reported in literature are based on impedance measurements, to identify a particular resonant frequency, or a frequency point that has a particular property such as a minimum of the phase. The measurement techniques are:
   a)   minimum phase measurement technique (Min-Phase),
   b)   three resonances (3-Resonances).

As reported in the following in this paragraph, the analysis of the two techniques leads to the conclusion that: the minimum phase measurement technique is simpler since it is requested to measure the minimum of a phase and the related conditioning circuit is simpler, but the measurement system operates at fixed distance. The technique of the three resonances is more complicated since it requires the measurement of three resonant frequencies and added electronic circuits to execute a formula but is able to compensate for variations in distance.

2.3.1 Min phase technique

One method, reported in (Harpster et al, 2002; Wang et al., 2008), measures the frequency at which the phase of the impedance reaches its minimum (Min-phase method). This frequency called f_{min} is shown in Figure 6. In the papers, the inductive telemetric systems consist of a planar inductance, in the sensing circuit, and a coil inductance, in the readout circuit. Considering the model reported in Figure 7, the readout circuit measures the impedance and the frequency at which the phase, in a short frequency interval, is at its minimum value (f_{min}); this frequency is related to the resonant frequency (f_0) of the sensing circuit that corresponds to:

$$f_0 = \frac{1}{2\pi\sqrt{L_S C_S}} \qquad (4)$$

In fact the total impedance, as seen from the terminals of the readout circuit, is given by:

$$Z_E(\omega) = R_1 + j\omega L_E + \frac{\omega^2 M^2}{Z_S(\omega)} \qquad (5)$$

In which the sensing circuit impedance Z_S is seen as reflected impedance to the readout impedance, with:

$$Z_S(\omega) = R_2 + j\omega L_S - j\frac{1}{\omega C_S} \qquad (6)$$

The total impedance reported in (5) can be rewritten considering the following expressions for the k (coupling coefficient) and Q (quality factor of the sensing circuit):

$$k = \frac{M}{\sqrt{L_E L_S}} \qquad (7)$$

$$Q = \frac{1}{R_2}\sqrt{\frac{L_S}{C_S}} \qquad (8)$$

Then, considering expression (4) the two following expressions can be derived:

$$L_S C_S = 1/\omega_0^2 \qquad (9)$$

$$R_2 = \omega_0 L_S / Q \qquad (10)$$

Substituting (7), (9), (10) and (6) in (5), the total impedance is given by:

$$Z_E(\omega) = R_1 + j\omega L_E \left[1 + k^2 \frac{\omega^2/\omega_0^2}{1 - \omega^2/\omega_0^2 + j\omega/\omega_0 Q} \right]$$ (11)

The phase of the impedance can be evaluated as:

$$\angle Z_E(\omega) = arctg \frac{Im(Z_E(\omega))}{Re(Z_E(\omega))}$$ (12)

To find the frequency at the phase minimum (f_{min}), equation (12) is first differentiated and then equated to zero, thus:

$$\frac{d\{ arctg[Im(Z_E(\omega))/Re(Z_E(\omega))] \}}{d\omega} = 0$$ (13)

The frequency at the phase minimum (f_{min}) is related by f_0 from the expression (14), which corresponds to the Taylor expansion of f_{min} in k (coupling coefficient) and Q^{-1} (quality factor of the sensing circuit) (Fonseca et al., 2002).

$$f_{min} = f_0 \left(1 + \frac{k^2}{4} + \frac{1}{8Q^2} \right)$$ (14)

The expression denotes that a distance change, considered equation (7), affects the coupling factor and consequently the f_{min}. This method is valid only in the interval near f_{min} and the self-resonance of the readout inductor is much higher.

2.3.2 The three resonances method
In the recent years a more accurate method has been reported in the literature. It measures all the three resonances and compensates the distance variation between the two inductors (3-Resonances Method) (Marioli et al., 2005).
This method is based on a parameter, called "F", whose value depends only on distance. According to the symbols reported in Figure 5, "F" parameter is defined equal to:

$$F = \frac{1}{C_1 \left(L_R + \frac{L_M L}{L_M + L} \right)}$$ (15)

"F" parameter derives from the sum of the squares of three resonant frequencies according to the following expression:

$$\left(2\pi f_{ra}\right)^2 + \left(2\pi f_{rb}\right)^2 - \left(2\pi f_a\right)^2 \tag{16}$$

Since from equations (3):

$$\left(2\pi f_{ra}\right)^2 + \left(2\pi f_{rb}\right)^2 = \frac{1}{C\left(L+\dfrac{L_R L_M}{L_R+L_M}\right)} + \frac{1}{C_1\left(L_R+\dfrac{L L_M}{L+L_M}\right)} \tag{17}$$

And from equation (2)

$$\left(2\pi f_a\right)^2 = \frac{1}{C\cdot\left(L+\dfrac{L_M L_R}{L_R+L_M}\right)} \tag{18}$$

It is immediate to demonstrate that:

$$\left(2\pi f_{ra}\right)^2 + \left(2\pi f_{rb}\right)^2 - \left(2\pi f_a\right)^2 = \frac{1}{C_1\left(L_R+\dfrac{L_M L}{L_M+L}\right)} \tag{19}$$

Or in other word:

$$F = \left(2\pi f_{ra}\right)^2 + \left(2\pi f_{rb}\right)^2 - \left(2\pi f_a\right)^2 = \frac{1}{C_1\left(L_R+\dfrac{L_M L}{L_M+L}\right)} \tag{20}$$

If C_1 is fixed, "F" depends only on coupled and leakage fluxes: these values are related only to the distance and not to the transducer capacitance. Moreover, the parameter "F" is obtained by a direct measurement since it can be calculated by elaborating the measurement of the three f_{ra}, f_{rb} and f_a resonant frequencies.
Introducing the following expressions:

$$L = L_S \cdot n^2 \tag{21}$$

$$C = \frac{C'_S}{n^2} \tag{22}$$

$$L_1 = L_R + L_M \tag{23}$$

and

$$L_2 = L_S + \frac{L_M}{n^2} \tag{24}$$

Substituting equations (21), (22), (23) and (24) into (18) and in (20) and re-arranging the expressions, the following expressions are obtained:

$$F = \cfrac{1}{C_1\left(L_R + \cfrac{L_M L_S \cdot n^2}{L_M + L_S \cdot n^2}\right)} = \cfrac{1}{\cfrac{C_1}{n^2}\left(\cfrac{L_R L_S \cdot n^2 + L_M L_S \cdot n^2 + L_M L_R}{L_2}\right)} \qquad (25)$$

$$(2\pi f_a)^2 = \cfrac{1}{\cfrac{C'_S}{n^2}\cdot\left(L_S \cdot n^2 + \cfrac{L_M L_R}{L_R + L_M}\right)} = \cfrac{1}{\cfrac{C'_S}{n^2}\cdot\left(\cfrac{L_R L_S \cdot n^2 + L_M L_S \cdot n^2 + L_M L_R}{L_1}\right)} \qquad (26)$$

The ratio of equation (25) with equation (26) is equal to:

$$\frac{F}{(2\pi f_a)^2} = \frac{L_2 C'_S}{L_1 C_1} \qquad (27)$$

Re-arranging (27), a straightforward expression of the sensor capacitance (C'_S) is:

$$C'_S = \frac{L_1 C_1}{L_2}\frac{F}{(2\pi f_a)^2} \qquad (28)$$

C'_S is obtained as a product between a constant term and a second one calculated from the three measured f_{ra}, f_{rb} and f_a frequencies. The constant term can be automatically obtained from a calibration or can be calculated measuring the equivalent circuit parameters of the each single planar inductor: L_1 and L_2 are the self-inductances of the read-out and sensing inductances, while C_1 is the parasitic capacitance (or any other added capacitance) of the readout circuit.

Equation (28) has been derived with no restricting hypothesis and maintains its significance also when the self resonance of the readout circuit is lower than f_0.

3. Measurement Circuit

In this paragraph, an electronics system that measures the three resonant frequencies and implements the 3-Resonances technique is presented.

The three resonant frequencies (f_{ra}, f_{rb} and f_a) are evaluated measuring the squared impedance module, in a defined frequency range, as seen from the terminals of the readout inductor, while the capacitance value of the sensor is calculated using equation (28) by a digital elaboration unit.

The module of the impedance is obtained applying a sinusoidal voltage to the inductor terminals and measuring the current flowing into. The sinusoidal current is subsequently squared and low-pass filtered such as to extract only the square of the amplitude value. Also the imposed voltage is squared and low-pass filtered such as to extract only the square of the amplitude value. The ratio between the squared modules of the imposed voltage and that of the measured current gives the squared impedance module. From this signal the value of the three resonant frequencies are recognized as minimum and maximum values: f_{ra} and f_a are the first maximum and minimum respectively, while f_{rb} is the second maximum.

An experimental circuit has been designed, fabricated and tested. A block diagram of this circuit is shown in Figure 8. In this scheme the telemetric system is reported as "Z-block".

The circuit consists of a block for the generation of the reference signal (synthesizer), of a block for the analysis of the impedance module (impedance analyzer) and of another block for the command and elaboration of the data (elaboration system). The synthesizer generates a sinusoidal variable-frequency signal (V_{DDS}) that drives the impedance analyzer module. The value of the frequency is controlled by the digital unit. The impedance module analyzer is driven by the signal coming from the synthesizer and gives a d.c. signal (V_{out}) proportional to the squared impedance module of the telemetric system.

The elaboration system acquires V_{out}, identifies f_{ra}, f_{rb} and f_a, and calculates C's according to equation (28).
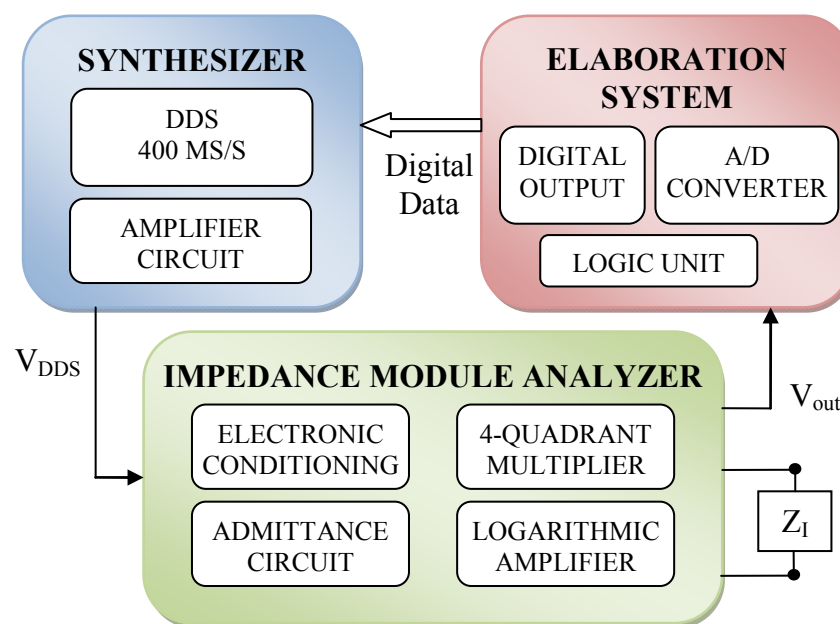
Fig. 8. A block scheme of the electronic circuit for resonant frequencies analyzer.

The synthesizer contains a DDS (Direct Digital Synthesizer), produced by Analog Device (AD9954). The elaboration system consists of a logic unit that drives the DDS, acquires the impedance module through the analog to digital converter, calculates the resonant frequencies and the C'_S value. For practical reason the elaboration system of the fabricated circuit consists of a PC equipped with an acquisition card of the National Instruments (PCI-6024E) and a dedicated software (LabVIEW), but a microcontroller could be used as well. The software LabVIEW controls the frequency and amplitude of the sinusoidal voltage generated by the synthesizer and subsequently samples the output signal V_{out}.
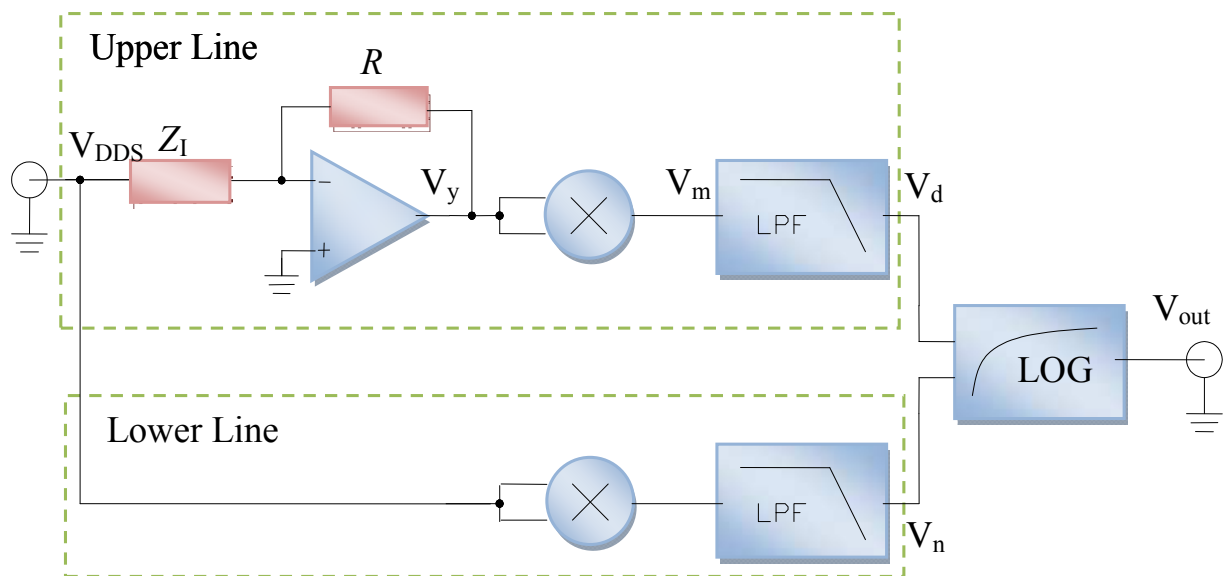
Fig. 9. Block diagram of the impedance module analyzer.

In Figure 9 the block diagram of the impedance analyzer is reported. The input signal V_{DDS} is the sinusoidal voltage generated by the synthesizer and represents the input of two different paths: the upper line and the lower line. In the upper line the readout inductor has one terminal connected to the input of the operational amplifier and the other is driven by the V_{DDS} signal coming from the DDS. The output V_y is proportional to the current, since Z_I is the impedance of telemetric sensor: V_y is proportional to the current flowing into the telemetric sensor, thus:

$$V_{\mathrm{y}} = -R\frac{V_{DDS}}{Z_I} = -RI \qquad (29)$$

Subsequently the signal is squared by a four-quadrant multiplier (AD835): V_m has a mean value proportional to the squared current module and a double frequency component. Then the third order low-pass filter extracts the d.c. value of the signal (V_d), thus:

$$V_{\mathrm{d}} = R^2|I|^2 = R^2\frac{|V_{DDS}|^2}{|Z_I|^2} \qquad (30)$$

Also V_{DDS} is elaborated and a signal V_n equal to the square module of V_{DDS} is obtained.

$$V_{\mathrm{n}} = |V_{DDS}|^2 \qquad (31)$$

The following block, using a logarithmic amplifier (LOG104) produced by Texas Instruments, calculates the difference of the logarithmic of V_n and V_d. The logarithmic amplifier permits also to implement the ratio between the voltage of the lower line and the current of the upper line, then the output is an impedance diagram. Since the difference

among two logarithms corresponds to the logarithm of the ratio, the signal V_{out} is proportional to the logarithm of the impedance Z_I.

$$V_{out} = \frac{1}{2} Log V_n - Log V_d = \frac{1}{2}\left(Log \frac{V_n}{V_d} \right) = \frac{1}{2} Log \frac{|V_{DDS}|^2 |Z_I|^2}{|V_{DDS}|^2 R^2} =$$
$$= \frac{1}{2} Log \frac{|Z_I|^2}{R^2} = Log |Z_I| - b$$

(32)

The impedance module of the telemetry system has wide variations and in order to keep the signals into the linear range of each block the V_{DDS} voltage can vary. Moreover V_{DDS} voltage can also slightly change due to problems of nonlinearity or temperature shift of the DDS circuit's output. The logarithmic block, according to equation (32), compensates for V_{DDS} change. Furthermore, the constant term b of equation (32) can be neglected because the resonant frequencies are evaluated as relative maximum and minimum quantities. The whole system has been tested in the laboratory applied to an inductive telemetric system for humidity measurement; several results are reported in the following paragraph (5).

4. An Inductive Telemetric System for Temperature Measurements

In this paragraph an inductive telemetric system measures high-temperature in harsh industrial environments. The sensing inductor is a hybrid device constituted by a MEMS temperature sensor developed using the Metal MUMPs process (Andò et al., 2008) and a planar inductor fabricated in thick film technology by screen printing over an alumina substrate a conductive ink in a spiral shape. The MEMS working principle is based on a capacitance variation due to changing of the area faced between the two armatures. The area changing appears as a consequence of a structural deformation due to temperature variation. The readout inductor is a planar inductor too.

 An impedance analyzer measures the impedance at the terminals of the readout inductor, and the MEMS capacitance value is calculated by applying the methods of the three resonances and minimum phase. Moreover, the capacitance value of similar MEMS is also evaluated by another impedance analyzer through a direct measurement at the sensing inductor terminals. The values obtained from the three methods have been compared between them.

The inductive telemetric system for high temperature measurement is shown schematically in Figure 10. On the left side of the figure a diagram of the inductive telemetric system is reported: the sensing element that consists of a planar inductor and a MEMS sensor is placed in an oven, while outside, separated by a window of tempered glass with a thickness of 8 mm, there is the readout inductor. The readout inductor was positioned axially to the hybrid sensor at about one centimetre to the hybrid sensor inside the chamber, while outside the readout was connected to the impedance analyzer. The two inductors represent an inductive telemetric system.
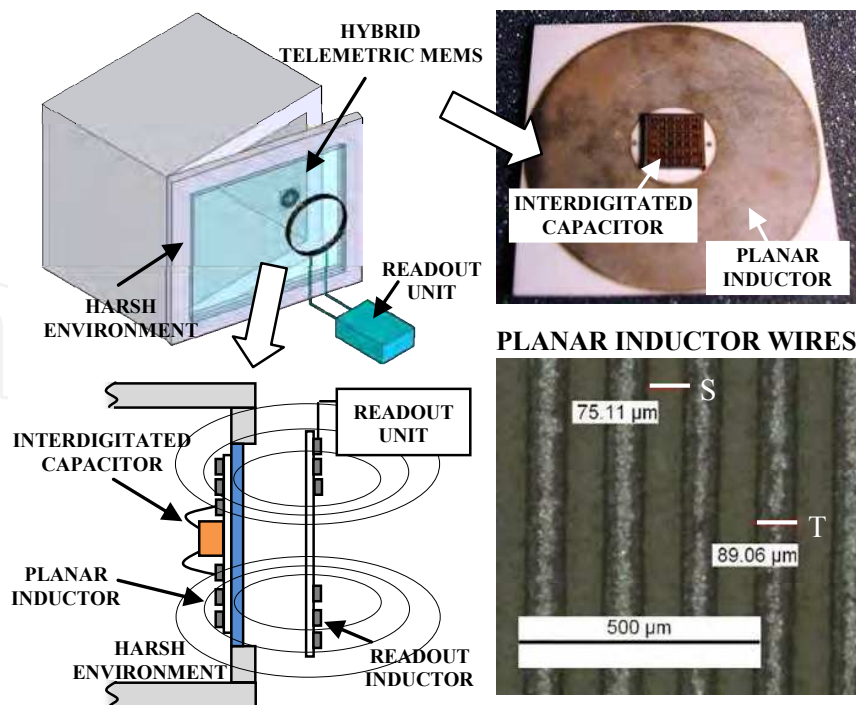
Fig. 10. The inductive telemetric system for high temperature measurement.

The planar inductor, reported on the right, has been obtained by a laser micro-cutting of a layer of conductive thick films (Du Pont QM14) screen printed over an alumina substrate (50 mm x 50 mm x 0.63 mm). The micro-cutting process consists of a material ablation by a laser. The inductor has the external diameter of 50 mm, 120 windings each of about 89 μm width and spaced 75 μm from the others: an enlargement is reported below on the left of Figure 10. The readout inductor is a planar spiral; it has been realized by a photolithographic technology on a high-temperature substrate (85N commercialized by Arlon). The readout inductor has 25 windings, each of 250 μm width and spaced 250 μm from the others. The internal diameter is 50 mm wide.

The experimental apparatus is schematically reported in Figure 11 and consists of an oven, three Fluke multimeters, three Pt100 references, two impedance analyzers, a PC and a power interface. In the measurement chamber (in the centre of the figure) an IR heater of 500 W rises the temperature up to 350 °C. Three Pt100 thermo-resistances (only one is shown in the Figure) measure the internal temperature in three different points, and each one is connected to a multimeter (Fluke 8840A). The three values are used to assure that the temperature is uniformly distributed.

A Personal Computer, over which runs a developed LabVIEW™ virtual-instrument, monitors the temperature inside the oven and controls the IR heater by turning alternatively on and off the power circuit. Two MEMS sensors are placed in the oven. The first one is directly connected to the impedance analyzer (HP4194A) to measure its capacitance; the second one is connected to the external readout inductor for the telemetric measurement. The experimental measurement has been conducted to a temperature up to 330 °C in a temperature-controlled measurement oven.
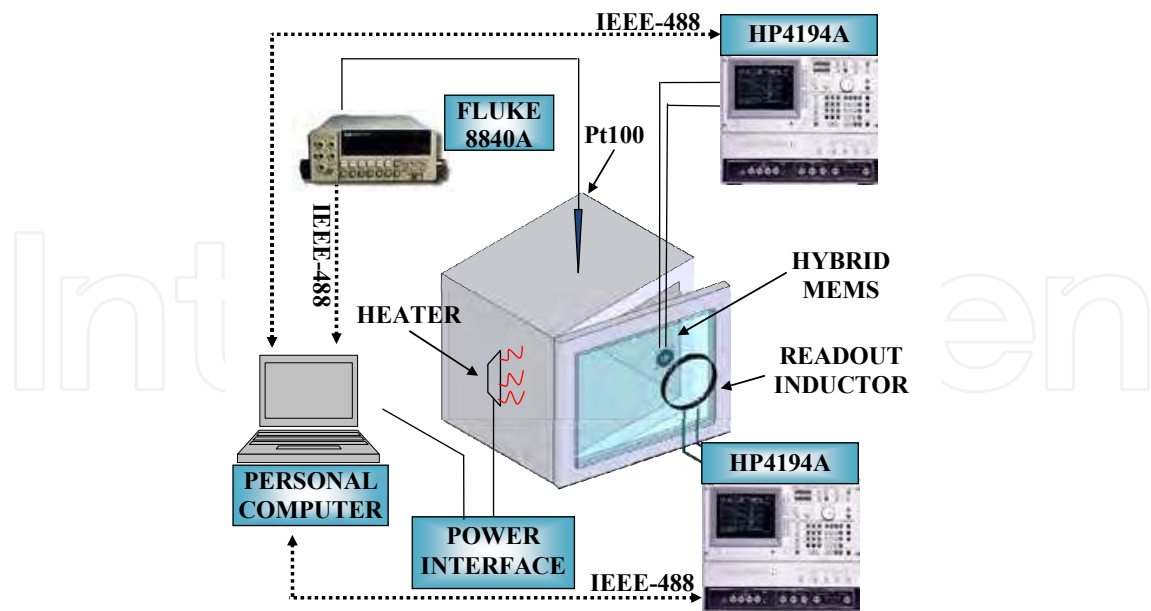
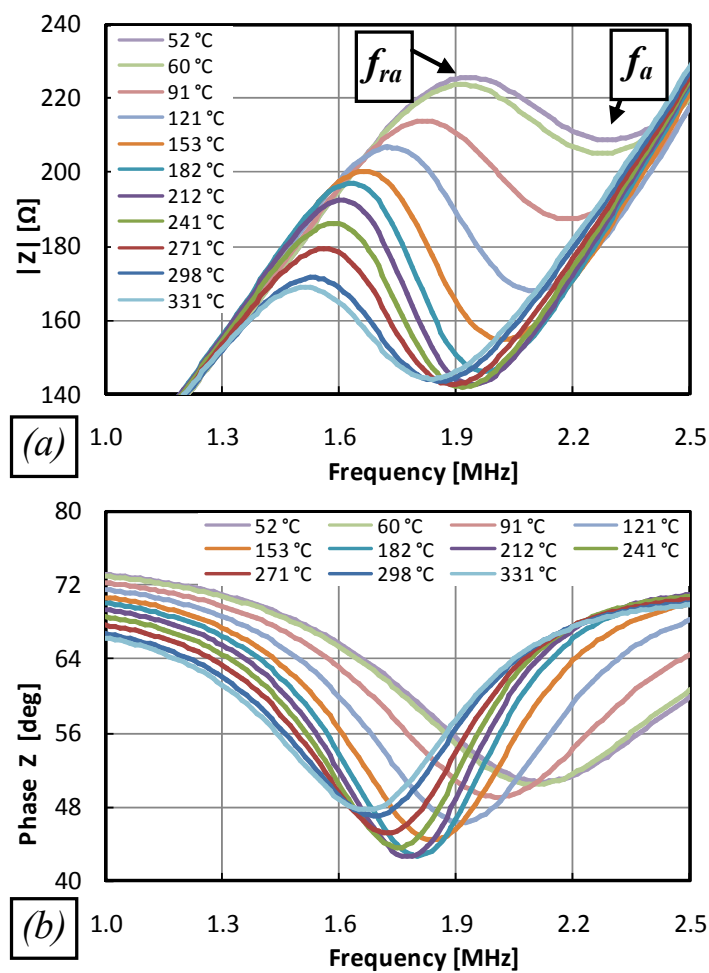Fig. 11. A diagram of the experimental setup.

Fig. 12. Modulus (a) and phase (b) of the hybrid MEMS measured with the impedance analyzer at different temperatures.

In Figure 12 modulus (a) and phase (b) diagrams of the impedance, as measured by the impedance analyzer at the readout terminal, for different temperatures are reported. The frequency interval of the abscissa has been chosen to make visible he resonant frequencies f_{ra}, f_a. As expected an increasing in temperature generates a decreasing of the values of the resonant frequencies, since the sensor capacitance value increases.

TEMP. [°C]	f_{ra} [MHz]	f_a [MHz]	f_{rb} [MHz]
52	1.9323	2.2904	4.9825
60	1.9120	2.2760	4.9883
91	1.8125	2.1866	4.9853
121	1.7348	2.1005	4.9783
153	1.6625	2.0146	4.9903
182	1.6308	1.9710	4.9928
212	1.6040	1.9414	4.9943
241	1.5828	1.9156	5.0053
271	1.5580	1.8918	5.0255
298	1.5328	1.8557	5.0285
301	1.5243	1.8798	5.0485
331	1.5130	1.8386	5.0463

Table. 1. Frequencies values of f_{ra}, f_{rb} and f_a measured for different temperatures.

In Table 1, f_{ra}, f_{rb} and f_a values are reported. The two frequencies f_{ra}, f_a, shown also in Figure 12, move down in frequency with increasing temperature as expected. The third frequency f_{rb} is sensitive to temperature, but less than the previous two.
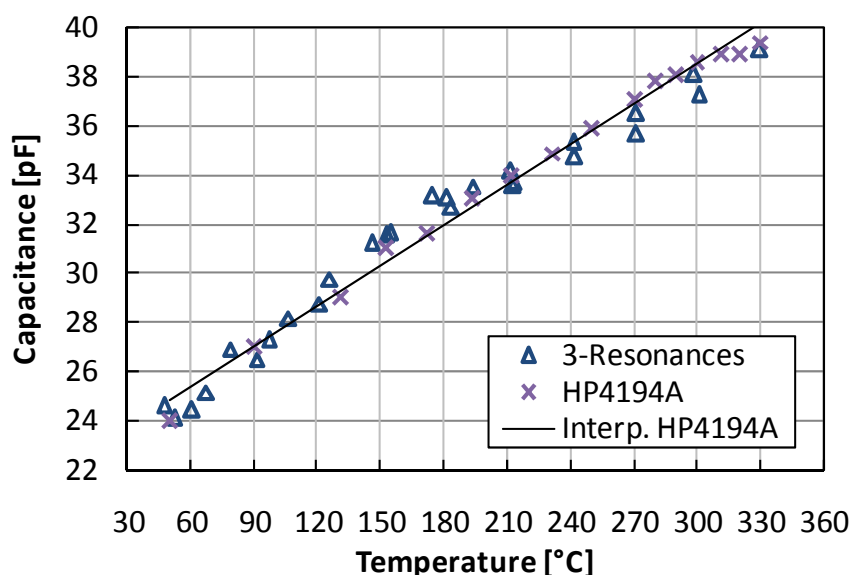
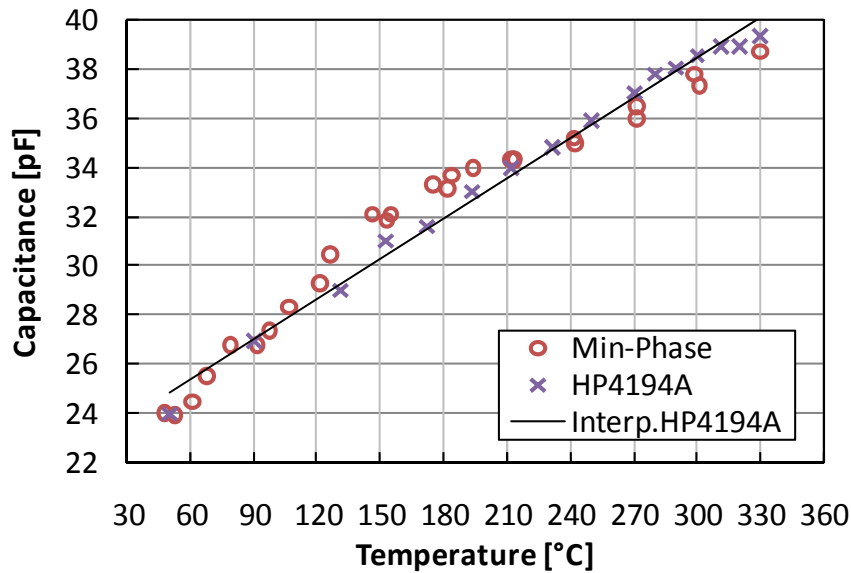Fig. 13. Sensor's capacitance is reported as a function of the temperature.

Fig. 14. Sensor's capacitance is reported as a function of the temperature.

In Figure 13 the sensor's capacitance is reported as a function of the temperature: cross points are the values directly measured on the sensor terminals, while the triangle are values calculated using the 3-Resonances method and measuring the impedance from the external inductor terminals. The straight line represents the linear interpolation of the data obtained by the impedance analyzer and it is reached as reference line. The calculated values using the 3-Resonances method (Figure 13) shows a quasi linear behaviour of the sensor: the maximum deviation is about 1.61 pF. Same consideration can be done for the data obtained using the Min-phase method: the maximum deviation is about 2.15 pF; a comparison is shown in Figure 14. Then, both the values calculated with the two methods are closely to the reference one measured with the impedance analyzer (HP4194A).
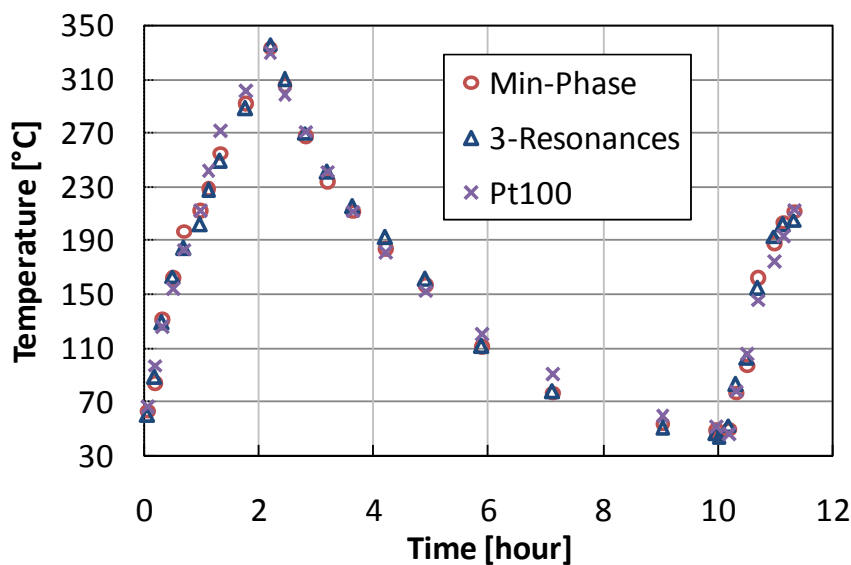
Fig. 15. Temperature values measured with the Pt100 and compared with the Min-Phase and 3-Resonances calculated values.

In Figure 15 the temperatures measured with the reference sensor (Pt100) are compared with the values calculated by the Min-Phase and 3-Resonances methods. The temperature values are obtained using the sensitivity of about 54.6 fF/°C, calculated using the linear interpolation previously reported. Figure 15 shows a good agreement of the temperature values during both the heating and the cooling process. The hybrid MEMS follows the trend of the temperature signal that it has estimated of about 1.9 °C/min and 0.6 °C/min during the heating and cooling process, respectively.

5. An Inductive Telemetric System for Relative Humidity Measurements

This paragraph describes a telemetric system to measure the relative humidity (RH). A telemetric system can be useful in hermetic environments since the measurement can be executed without violating the integrity of the protected environment.

The telemetric system presented here has an interesting characteristic: the sensing inductor does not have any transducer, since the parasitic capacitance of the sensing inductor is the sensing element. In this paragraph, the measurement technique of the three resonances has been used to analyse the effectiveness of compensation in the distance.

In this system the sensing inductor consists only of the planar inductor over which a polymer, humidity sensitive, is deposited. This polymer is sensitive to the humidity and changes its dielectric permittivity causing a variation of the inductor parasitic capacitance. The terminals of the readout inductor are the input of the conditioning electronics reported in paragraph 3. The electronics measures the frequency resonances, extracts the corresponding capacitance values and compensates the distance variation as well.
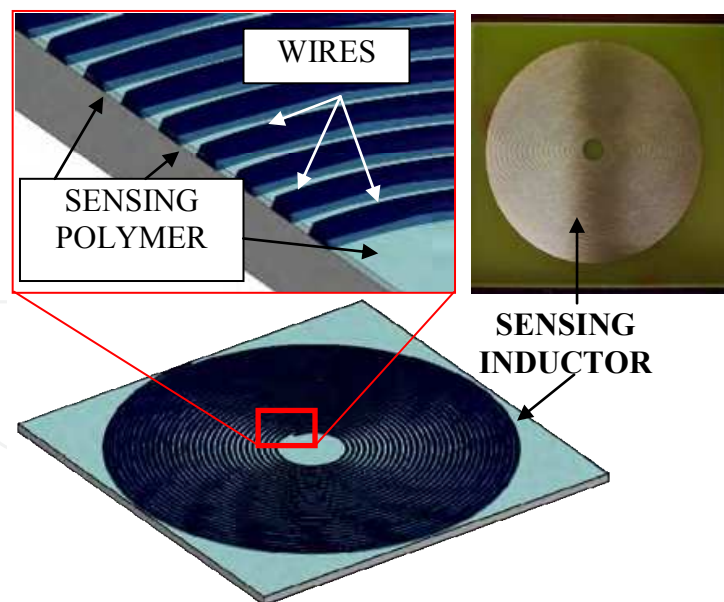

Fig. 16. The inductive sensor, on which a polymer, humidity sensitive, is deposited.

In Figure 16 the passive inductive sensor is reported, which is a standalone planar inductor, fabricated in PCB technology of 25 windings with an external diameter of 50 mm covered by polyethylene glycol (PEG). Polyethylene glycol (PEG) was chosen for the highest sensitivity, but other polymer sensitive to the RH can be used as well. Differently from the others tested

in laboratory, this polymer is soluble in water: this characteristic influences the sensitivity positively, but increases the hysteresis as well. Its dielectric constant changes from 2.2 to 4 and depends on temperature and humidity. The characteristics of the telemetric system have been verified with a humidity-controlled hermetical measurement chamber changing also the distance between the sensing and readout inductors.
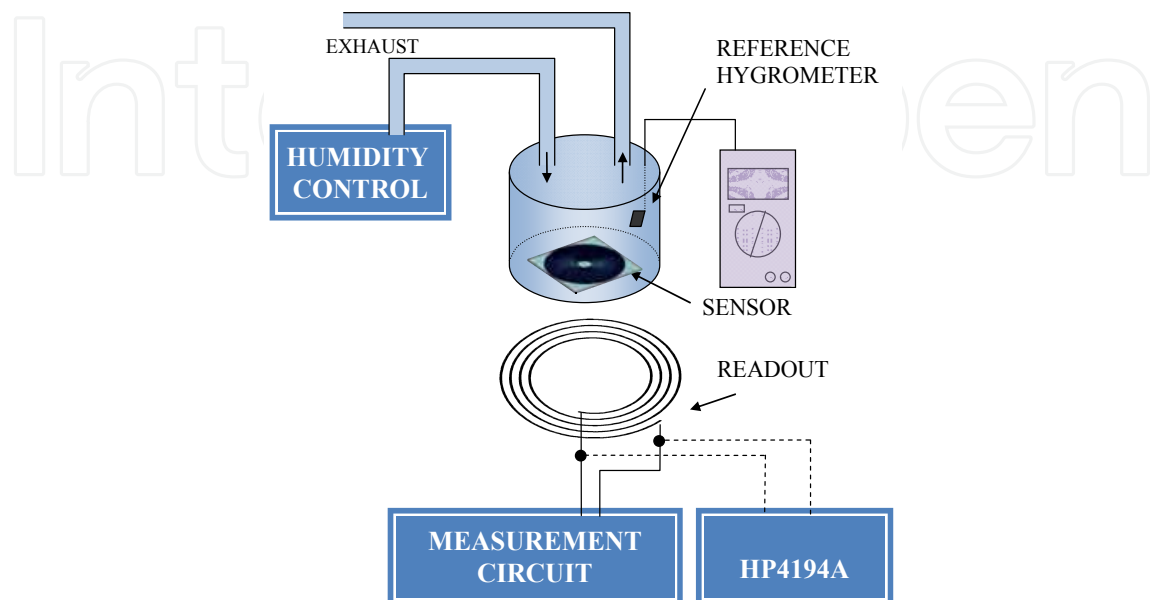

Fig. 17. Block scheme of the experimental system.

In Figure 17 the experimental apparatus to test the telemetric system is schematically represented. The sensor is positioned inside a Plexiglas chamber, which is used as a hermetic container for the damp air. Two pipes are linked to the measurement chamber, one of which introduces controlled damp air. The damp air is produced by a system that compounds dry air and wet air using two flux-meters. The time required to reach the new RH value is about one hour and half. In the chamber there is a hygrometric sensor (HIH-3610 Honeywell) for reference measurements. The inductances are positioned parallel and their axes are coincident. The distance of the readout from the sensor is controlled by a micrometric screw with resolution 10 µm and runs up to 25 mm. The terminals of the readout inductor are connected to the input of the conditioning electronics or, alternatively, to the input of the impedance analyzer. The use of the impedance analyzer is used only for test purposes. The proposed electronics measures the frequency resonances and calculates the corresponding capacitance values according to formula (28). The formula compensates the distance variation as well.

The capacitance values measured at a distance of 20 mm between the readout and sensing inductors the calculated capacitance values are reported in Figure 18: the square point are the value obtained by the electronics while the values obtained using the impedance analyzer (HP4194A) are reported as cross points. All the measurement points are a function of the RH values as measured by the reference sensor. Interpolating the two sets of measurement data the maximum difference between the two curves is less than 15 fF, corresponding to less than 8% of the capacitance measurement range.

In Figure 19 the capacitance values as a function of distance are reported over a distance variation from 15 to 30 mm. The maximum variation of the capacitance is, in the worst case, limited to 20 fF corresponding to about of 1% of FS for each millimetre of distance variation.
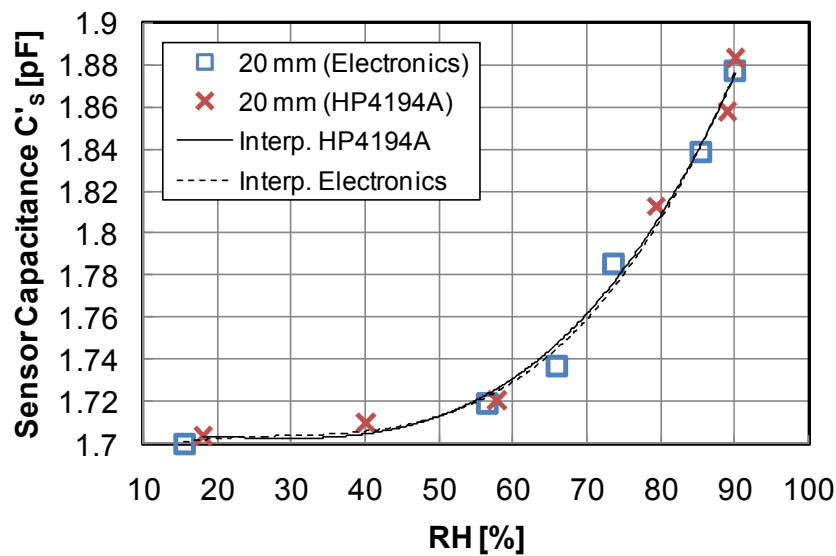
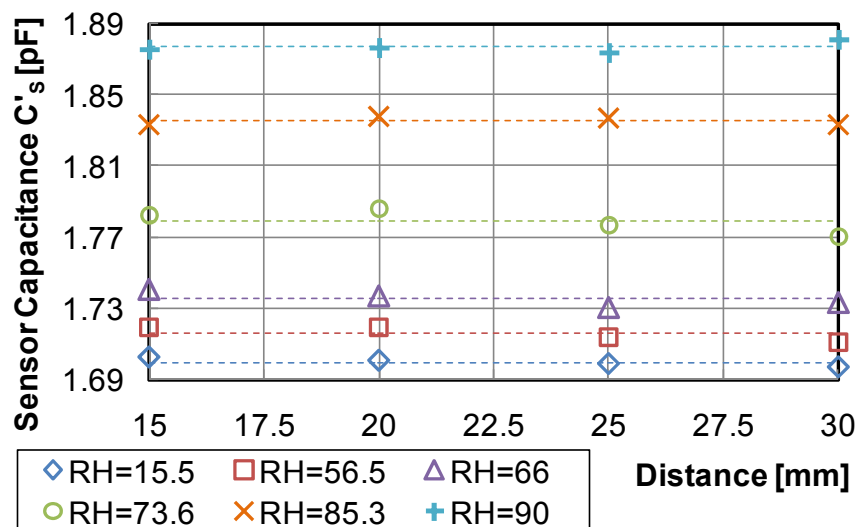Fig. 18. The calculated capacitance values as a function of RH and for different distance values.

Fig. 19. The capacitance values as a function of distance for different RH values.

6. Conclusion

Inductive telemetric systems offer solutions to specific applications where the measurement data should be acquired in environments that are incompatible with the active electronics or are inaccessible. They also work without batteries, consequently reducing the problem of environmental impact. The general architecture of an inductive telemetric system, the measurement techniques, commonly used, were presented, along with the description of developed telemetric systems applied in harsh or hermetic environments. Two examples of passive inductive telemetric systems were reported, the first one for humidity measurements which presents a distance interval of about 30 mm and the possibility to compensate the distance variation. The second one can measure high temperatures with a maximum limit of about 350 °C, guaranteeing the inviolability of the harsh environment.

7. References

Akar, O.; Akin, T. & Najafi, K. (2001). A wireless batch sealed absolute capacitive pressure sensor, *Sensors and Actuators A,* Vol. 95 pp. 29-38.

Andò, B.; Baglio, S.; Pitrone, N.; Savalli, N. & Trigona, C. (2008). Bent beam MEMS temperature sensors for contactless measurements in harsh environments, *Proceedings of IEEE I2MTC08*, Victoria BC, Canada, pp. 1930-1934.

Birdsell, E. & Allen, M.G.; (2006). Wireless Chemical Sensors for High Temperature environments, *Tech. Dig. Solid-State Sensor, Actuator, and Microsystems Workshop*, Hilton Head Island, SC, USA, pp. 212-215.

Fonseca, M.A.; Allen, M.G.; Kroh, J. & White, J. (2006). Flexible wireless passive pressure sensors for biomedical applications, *Tech. Dig. Solid State Sensor, Actuator, and Microsystems Workshop*, Hilton Head Island, South Carolina, June 4-8, pp. 37-42.

Fonseca, M.A.; English, J.M.; Von Arx, M. & Allen, M.G. (2002). Wireless micromachined ceramic pressure sensor for high temperature applications, *Journal of Microel. Systems*, Vol. 11, pp. 337-343.

Hamici, Z.; Itti, R. & Champier, J. (1996). A high-efficiency power and data transmission system for biomedical implanted electronic device, *Measurement Science and Technology*, Vol. 7, pp. 192-201.

Harpster, T.; Stark, B. & Najafi, K. (2002). A passive wireless integrated humidity sensor, *Sensors and Actuators A*, Vol. 95, pp. 100-107.

Jia, Y.; Sun, K.; Agosto, F.J. & Quinones, M.T. (2006). Design and characterization of a passive wireless strain sensor, *Measurement Science and Technology*, Vol. 17, pp. 2869-2876.

Marioli, D.; Sardini, E.; Serpelloni, M. & Taroni, A. (2005). A new measurement method for capacitance transducers in a distance compensated telemetric sensor system, *Measurement Science and Technology*, Vol. 16, pp. 1593-1599.

Ong, K.G.; Grimes, C.A.; Robbins, C.L. & Singh, R.S. (2001). Design and application of a wireless, passive, resonant-circuit environmental monitoring sensor, *Sensors and Actuators A*, Vol. 93, pp. 33-43.

Schnakenberg, U.; Walter, P.; Vom Bogel G.; Kruger C.; Ludtke-Handjery H.C.; Richter H.A.; Specht W.; Ruokonen P. & Mokwa W. (2000). Initial investigations on systems for measuring intraocular pressure, *Sensors and Actuators A,* Vol. 85, pp. 287-291.

Takahata, K. & Gianchandani, Y.B. (2008). A micromachined capacitive pressure sensor using a cavity-less structure with bulk-metal/elastomer layers and its wireless telemetry application, *Sensors*, Vol. 8, pp. 2317-2330.

Tan, E.L.; Ng, W.N.; Shao, R.; Pereles, B.D. & Ong, K.G. (2007). A wireless, passive sensor for quantifying packaged food quality, *Sensors*, Vol. 7, pp. 1747-1756.

Todoroki, A.; Miyatani, S. & Shimamura, Y. (2003). Wireless strain monitoring using electrical capacitance change of tire: part II-passive, *Smart Materials and Structures*, Vol. 12, pp. 410-416.

Wang, Y.; Jia, Y.; Chen, Q. & Wang, Y. (2008). A Passive Wireless Temperature Sensor for Harsh Environment Applications, *Sensors*, Vol. 8, pp. 7982-7995.

Advances in Measurement Systems

Edited by Milind Kr Sharma

How to reference

In order to correctly reference this scholarly work, feel free to copy and paste the following:

INTECH
open science | open minds